Prognostic association of immunoproteasome expression in solid tumours is governed by the immediate immune environment

Rahul Kumar[1,3], Bhavya Dhaka[1,3], Sarthak Sahoo[2], Mohit Kumar Jolly[2], Radhakrishnan Sabarinathan[1,*]

[1]National Centre for Biological Sciences, Tata Institute of Fundamental Research, Bengaluru, 560065, India.
[2]Centre for BioSystems Science and Engineering, Indian Institute of Science, Bangalore 560012, India.
[3] These authors contributed equally to this work.

[*]Correspondence: sabari@ncbs.res.in

Abstract

Induction of immunoproteasome (IP) expression in tumour cells can enhance antigen presentation and immunogenicity. Recently, overexpression of IP genes has been associated with better prognosis and response to immune checkpoint blockade (ICB) therapies in melanoma. However, the extent of this association in other solid tumour types and how that is influenced by tumour cell-intrinsic and cell-extrinsic factors remains unclear. Here, we address this by exploring the gene expression patterns from bulk and single-cell transcriptomics data of primary tumours (from TCGA and other studies, respectively). We find that the IP expression positively correlates with the constitutive proteasome (CP) across multiple tumour types. Interestingly, both CP and IP are highly expressed in tumour cells closer to the tumour border than the core region. Furthermore, tumours with high IP expression exhibit cytotoxic immune cell infiltration and upregulation of interferon-gamma, TNF alpha and inflammatory response pathways in tumour cells. However, the association of IP expression with overall survival (in TCGA cohort) and response to ICB therapy (in non-TCGA cohorts) is tumour-type specific and is greatly influenced by the immune cell infiltration patterns. The overall survival is better in skin melanoma, breast carcinoma, bladder carcinoma, cervical squamous cell carcinoma, sarcoma, and mesothelioma; while it is poor in uveal melanoma, low-grade glioma

and kidney renal clear cell carcinoma. Similarly, the response to ICB therapy is better in skin melanoma, non-small cell lung cancer, breast cancer and thymic carcinoma, while it is worse in oral cancer and renal carcinoma. Together, this suggests that the IP expression combined with the immune infiltration patterns can be used as a biomarker to predict prognosis and response to ICB therapies in solid tumours.

Introduction

Proteasomes are an essential component of the ubiquitin-proteasome system that maintains protein homeostasis by degrading unwanted or misfolded proteins into smaller peptides. These peptides are then processed by the antigen-processing machinery and presented on the cell surface by the Major histocompatibility complex (MHC) class I molecules for immune surveillance (1,2). The proteasome complex (26S) constitutes one catalytic core (20S) and two terminal regulatory subunits (19S). The proteasome exists primarily in two forms: constitutive proteasome (CP) and immunoproteasome (IP) (and sometimes in an intermediate form as well) (2–4). The CP is ubiquitously expressed across all nucleated cell types, and its 20S core contains three catalytic cleaving subunits: β5/PSMB5 (chymotrypsin-like), β1/PSMB6 (caspase-like), and β2/PSMB7 (trypsin-like). Whereas in the IP (or 20Si), which are predominantly expressed in immune cells (e.g., antigen-presenting cells), the above three subunits are replaced by β5i/PSMB8 (chymotrypsin-like), β1i/PSMB9 (chymotrypsin-like), and β2i/PSMB10 (trypsin-like) (2–4).

In non-immune cells, the expression of IP genes can be induced by exposure to specific proinflammatory cytokines such as interferon-gamma (IFN-γ) and tumour necrosis factor alpha (TNF-α) under stress or inflammatory conditions (4). Following that, the replacement of CP with IP at the protein level is mediated by proteasome maturation protein (POMP) which favours the incorporation of the IP subunit due to its faster assembly (~4 fold faster) than CP (5–7). The IP has been shown to generate a higher immunogenic spectrum of peptides due to its altered cleavage site preferences (~32% unique sites as compared to CP) and also a higher number of spliced peptides (81%) than CP (65%) (2,8,9). This can lead to enhanced antigen presentation and thereby trigger the immune response. Genetic alterations and expression dysregulation of single or multiple subunits of IP have been associated

with reduction of MHC class I expression (in non-immune cells), loss of B-cells, defects in T-cell development and T helper cell differentiation, cytokines dysregulation, and reduced number of antigen-specific CD8+ T cells (10–13).

Although the role of IP expression and its prognostic association has been extensively studied in haematological malignancies (14,15), minimal studies have explored it in the context of solid tumours (see review (16)). A recent study in melanoma has shown that the overexpression of IP subunits (PSMB8 and PSMB9) was associated with improved survival and better response to anti-CTLA-4 and anti-PD-1 immunotherapies (17). Similarly, in breast cancer, the interferon-gamma mediated higher expression of IP was associated with better prognosis (18). In non-small cell lung cancer (NSCLC), patients with higher PSMB9 expression showed better response to anti-PD1 and progression-free survival (19). However, the extent of this association in other solid tumour types, and the influence of tumour cell-intrinsic and cell-extrinsic factors, remains unclear. Thus, in this study, we set out to address the following questions: (a) how CP and IP gene expression are (dys)regulated in tumours (that is, when the IP genes are induced what happens to the CP expression); (b) what proportion of the cells are expressing CP and IP within the tumour; (c) what tumour cell-intrinsic and cell-extrinsic factors influence the expression of CP and IP; and d) how does that affect the prognostic association and response to immune checkpoint blockade (ICB) therapies.

Through the gene expression analysis of bulk and single-cell transcriptomics data of primary tumour samples (from TCGA and other studies, respectively), we show that (a) the expression of IP and CP was positively correlated in multiple tumour types as compared to normal tissues; however, the expression of IP was relatively lower than CP in both tumours and normals; (b) the expression of IP was not only predominant in immune cells infiltrating the tumours, but also in the subset of tumour epithelial cells (around 33% of the total epithelial cells). Notably, the tumour epithelial cells located in the tumour border expressed higher IP and CP than those in the tumour core regions; (c) the expression of IP was positively correlated with the upregulation of hallmark pathways such as interferon-gamma response, interferon-alpha response, IL-6-JAK/STAT3 signalling, Reactive oxygen species (ROS) pathway;

while it was negatively correlated with upregulation of Wnt beta-catenin signalling, TGF-beta signalling and Hedgehog signalling; (d) the enrichment of cytotoxic immune infiltrating cells (such as activated CD8+ T-cells, Gamma delta T-cells and Natural killer cells) in the tumour microenvironment were positively correlated with higher expression of IP in tumour cells, whereas for eosinophils and T-helper cells, it was negatively correlated; (e) the association of IP expression with overall survival and response to ICB therapies was tumour type-specific and it was greatly influenced by the immune cell infiltration patterns (pro- or anti-tumorigenic). Taken together, these results suggest that the expression of IP in tumour cells can be influenced by both cell-intrinsic and cell-extrinsic factors. Thus, the expression of IP subunits combined with tumour immune cell infiltration patterns can be used as a better predictor of prognosis and response to ICB therapies in solid tumours besides skin melanoma.

Results

Immunoproteasome expression is higher in tumours than normal tissues

To study the expression patterns of the constitutive proteasome (CP) and immunoproteasome (IP), we first compared the average expression scores of genes encoding the catalytic subunits of CP (PSMB5, PSMB6, and PSMB7) and IP (PSMB8, PSMB9, and PSMB10) in 9,491 TCGA tumour samples, across 33 cancer types (see Methods, Supplementary Table 1). For most solid tumour types, we observed a significantly ($P<0.05$) higher expression of CP as compared to IP (Figure 1A). A similar trend was observed when controlled for tumour purity (>=70%) to reduce the confounding effects from the stromal and immune microenvironment (Supplementary Figure 1). However, in the tumours of hematopoietic origin – diffuse large B-cell lymphoma (DLBC) and acute myeloid leukemia (LAML) – a higher IP to CP expression was observed, which can be explained by the innate IP expression in hematopoietic cells. As compared to CP, the expression of IP was highly variable (large interquartile ranges) within each tumour type (Figure 1). This could be due to the influence of tumour cell-intrinsic and/or cell-extrinsic factors (which we have investigated in the sections below). Nevertheless, we observed a positive correlation

between CP and IP expression in multiple cancer types, suggesting that the induction of IP expression does not hinder CP expression in tumours (Figure 1A).

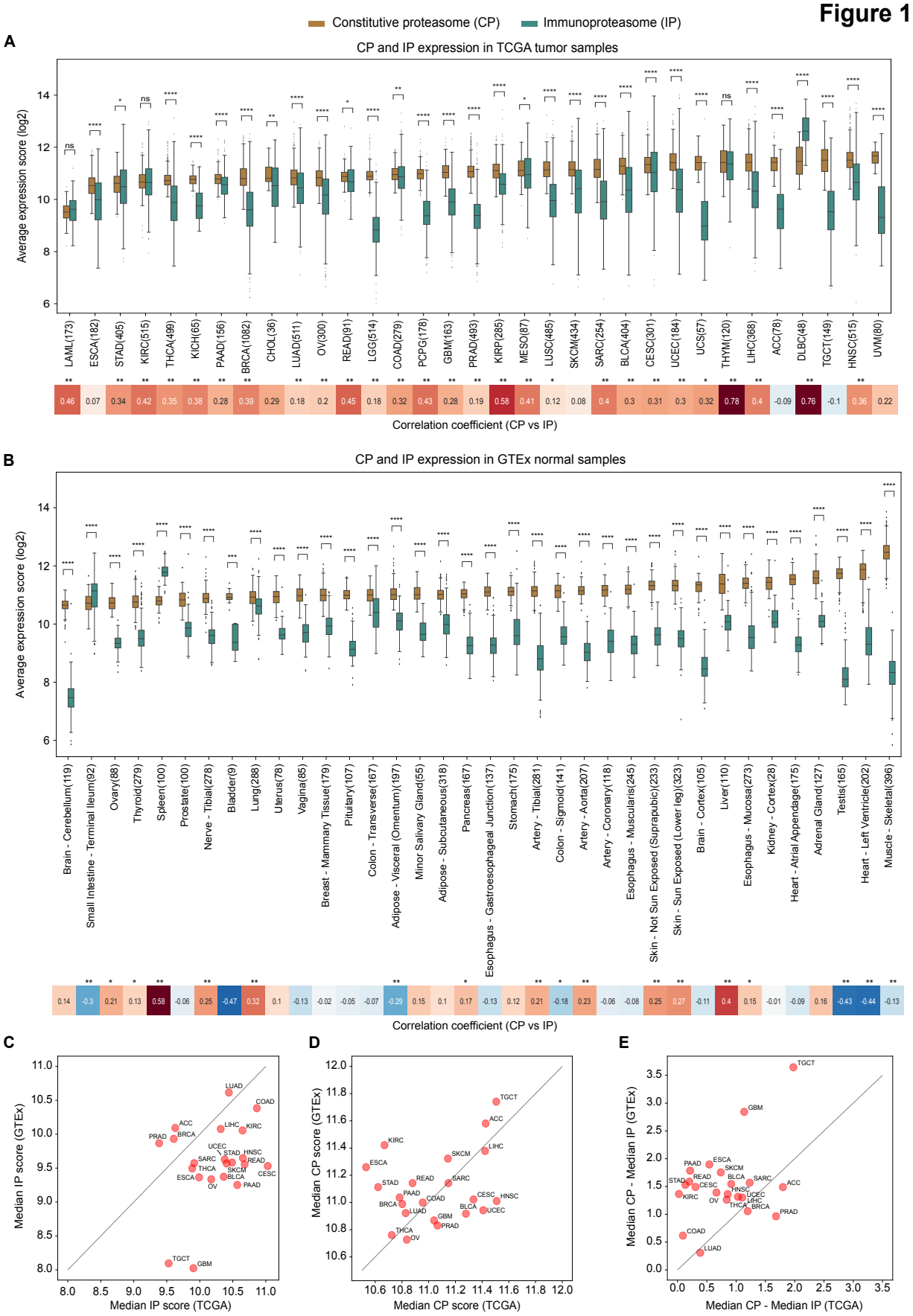

Figure 1: Comparison of CP and IP expression in tumours and normal tissues

A. The boxplot represents the distribution of gene expression levels of constitutive proteasome (CP) and immunoproteasome (IP) across multiple tumour tissues from TCGA. The x-axis represents the tumour tissues (and the number of samples) and the y-axis represents the log2 average expression (RSEM+1) of core genes of CP (PSMB5, PSMB6 and PSMB7) and IP (PSMB8, PSMB9 and PSMB10) (see Methods). The P-values were computed using Mann-Whitney U test (two-sided) and the significance level was represented as * $p<0.05$,** $p<0.01$ or ns - non-significant ($P>=0.05$). The heatmap at the bottom represents the Spearman's rank correlation between CP and IP expression and the asterisks symbol on the top indicates the P-value (with the significance level as mentioned above).

B. Same as A, but for the normal tissues from GTEx. The x-axis represents the normal tissues (and the number of the samples) and the y-axis represents the log2 average expression (RSEM+1) of CP and IP genes (as mentioned in A).

C. Comparison of the IP expression in TCGA tumour versus matched GTEx normal tissues. The value on the x- and y-axis represents the median of the average expression value of IP from the respective tissue type from tumour and GTEx, respectively.

D. Same as C, but for the CP.

E. Comparison of the difference in the average expression scores of CP and IP in TCGA tumours versus matched GTEx normal tissues.

Further, to compare the proteasome expression in a nonmalignant state we leveraged 6,125 GTEx samples across 36 tissue types (see Methods). Similar to TCGA tumours, most of the tissue types show significantly ($P<0.05$) higher expression of CP compared to IP (Figure 1B). As expected, the spleen and small intestine had increased IP expression, likely due to the enrichment of lymphocytes in the spleen and inflammation-induced IP expression in epithelial cells in the small intestine (15). However, the positive correlation between CP and IP expression was now only observed in specific tissue types (such as Liver, Lung, and Spleen).

Next, to quantify the tumour-driven nature of the proteasomes, we compared the median proteasome expression between tumours (TCGA) and corresponding normal tissues (GTEx) (Figure 1C-E). The IP expression was higher in tumours as compared to matched normal tissues, particularly in cervical (CESC), head-and-neck (HNSC), rectum adenocarcinoma (READ), and bladder adenocarcinoma (BLCA) (Figure 1C). However, this difference was minimal for CP (Figure 1D). Moreover, the median expression difference between the CP and IP was much lesser in tumours compared to the matched normal tissues (Figure 1E), as shown above (Figure 1A, B). Taken together, these results suggest that the IP expression is higher in tumour tissues as compared to normal tissues, however, with large variability within and across tumour types.

Immunoproteasome expression is variable among tumour epithelial cells

To delineate the relative contributions of tumour epithelial cells and infiltrating immune cells to the observed CP and IP expression patterns, we explored the publicly available single-cell gene expression data of nine tumour types (see Methods, Supplementary Table 2). As expected, the CP was expressed more in epithelial cells and IP in immune cells (Figure 2A-C, Colorectal cancer SMC cohort from (20)). Similar to TCGA tumours (bulk RNA-seq), we observed a significantly ($P<0.0001$) higher CP expression as compared to IP in epithelial cells in all nine cancer types (Figure 2D). Further, in the colon adenocarcinoma (KUL3 cohort from (20)), where tumour site information was available, we observed that the epithelial cells near the tumour border have higher proteasome expression than cells from the tumour core (median expression fold difference of 1.5 and 2 for CP and IP, respectively) (Figure 2E). This could be due to the higher exposure of tumour cells to the immune cells at the tumour border. In the tumour epithelial population, we also observed a strong positive correlation between the IP and CP expression (Figure 2F, Supplementary Figure 2A), similar to that of bulk transcriptomics data (Figure 1A).

Further, we asked what proportion of the tumour epithelial and immune cells express CP and IP. To check this, we selected tumour types annotated with immune cell population and estimated the proportion of cells expressing proteasome expression above the median level (see Methods) within each group (Figure 2G). This showed that across tumour types, only a subset of tumour epithelial cells (range 18-50%, mean 33%) expressed IP, whereas the majority of the T-cell (range 47-72%, mean 61%) and B-cell (range 23-71%, mean 49%) expressed IP. However, an opposite trend was observed with the CP expression. Taken together, these results suggest that the predominant IP expression is seen only in a subset of the tumour cells (~33%). Also, the expression level varies among the tumour cells with respect to their spatial distribution (tumour border vs core).

Figure 2

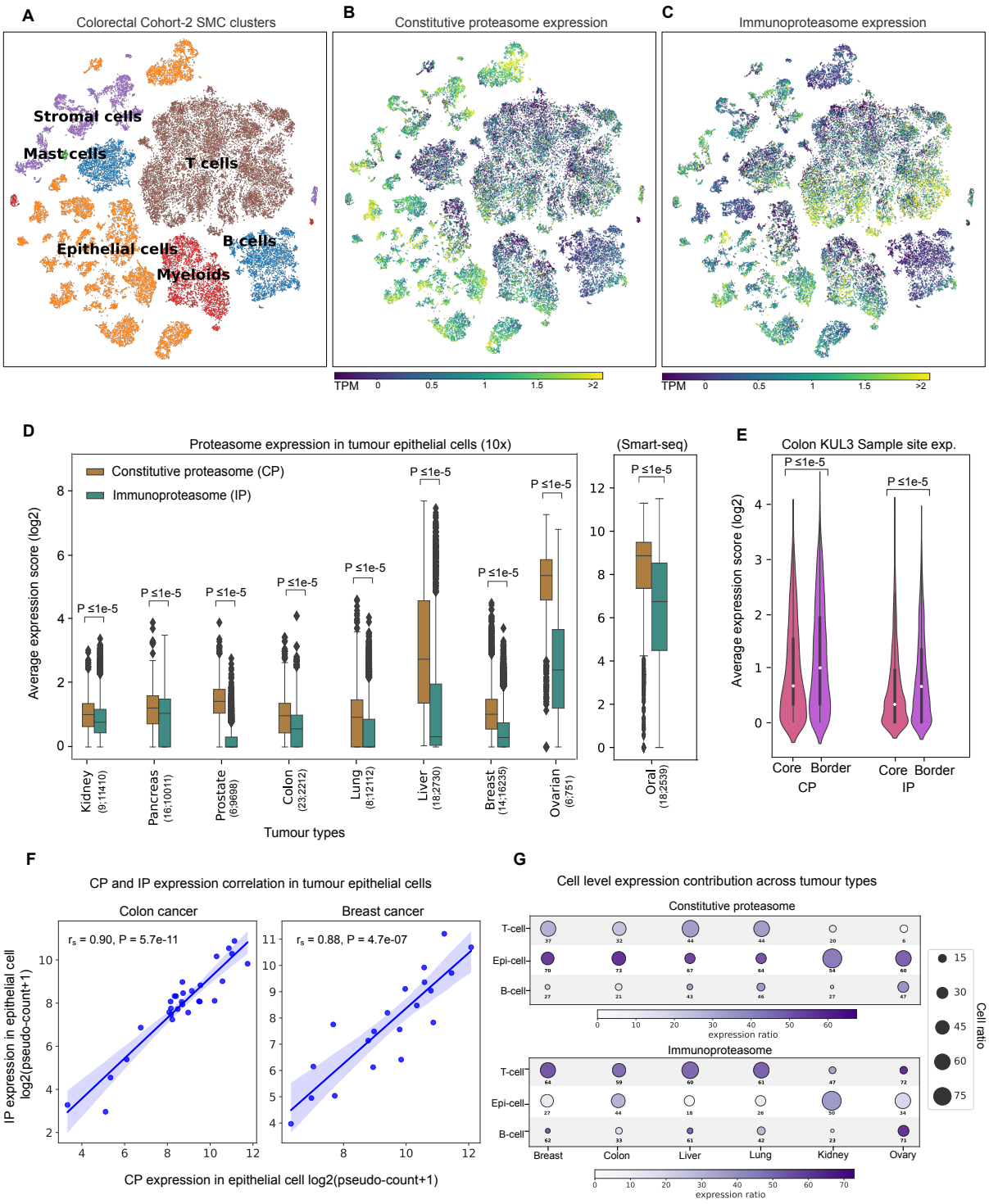

Figure 2: Single cell analysis of CP and IP expression in tumour epithelial and immune cells

A. The t-SNE plot shows the single cell gene expression data from colorectal cancer. Each dot represents a cell and the colour indicates the cell type annotation (epithelial cells, myeloid cells, B cells, T cells, Mast cells, or stromal cells).

B and **C** show the average expression of CP and IP, respectively, at the single cell level.

D. Distribution of average expression scores of proteasomes in tumour epithelial cells. The x-axis represents the tumour type and the values within the bracket indicates the number of patients and the number of individual cells considered. The y-axis represents the log2 average expression of CP and IP genes. The P-values were calculated using Mann-Whitney U test (one-sided).

E. Distribution of average expression scores of CP and IP in tumour epithelial cells with respect to tumour site information – border versus core (represented on x-axis) – in colon adenocarcinoma. The P-values were calculated using Mann-Whitney U test (one-sided).

F. Spearman's rank correlation between the average expression of CP and IP genes (from tumour epithelial cell population) in colon and breast cancers. Each dot represents a sample and the values on the x- and y-axis represent the proteasome expression as pseudo-count (i.e., average expression of CP or IP genes across all cells within the sample).
G. CP and IP expression level in T-cell, tumour epithelial cell and B-cell population. The size of the circle represents the abundance of the respective cell type in the total cell population under each tumour type. And, the colour inside (and the value mentioned below) represents the percentage of cells having expression value greater than the median expression value in that respective cell type.

Tumours with high immunoproteasome expression are enriched with anti-tumorigenic immune cells

To study the impact of tumour infiltrating immune cells (TIL) on the expression of CP and IP, we performed a differential analysis of enrichment of 18 different types of immune cells between high (top quartile) and low (bottom quartile) proteasome expression groups for each tumour type, by using GSVA (see Methods, Supplementary Table 3). With the absolute enrichment score difference > 0.2 and FDR (q-value) < 0.1, we found the enrichment of activated CD8+ T cells, activated dendritic cells (aDC), cytotoxic cells (which includes genes that are highly expressed in activated CD8+ T cells, gamma delta T cells and natural killer cells) and exhausted T cells in high IP groups across multiple cancer types (Figure 3A). These immune cells are known to produce inflammatory cytokines (IFN-γ and TNF-α) that can induce the IP expression in tumour cells. The enrichment of exhausted T-cells in high IP groups could be explained by persistent antigen-presentation and chronic inflammation in the tumour microenvironment (TME) (21). Although the regulatory T-cells (Tregs) are known to cause an immunosuppressive environment (22), the positive enrichment observed for certain tumour types here could be explained by involvement of PSMB8 expression in promoting Treg differentiation from CD4+ T-cells (12). We also observed a positive enrichment of activated dendritic cells (aDC) compared to immature dendritic cells (iDC) in multiple tumour types (Figure 3A). This could be due to the induction of IP during the dendritic cell activation process (23,24). On the other hand, the eosinophils and T-helper cells were negatively enriched in the high IP expression group.

In the case of CP, the gamma-delta T-cells showed a positive enrichment (Figure 3B) across tumour types, likely because of the extensive repertoire of these cells within the epithelial tissues (25). Similar to the IP, the activated CD8+ T cells and cytotoxic cells were positively enriched in the high CP group in multiple tumour types (Figure 3B), consistent with the expression correlation observed between CP and IP in bulk

(Figure 1A) and single-cell gene expression analysis (Figure 2F). The central memory T (Tcm) cells were negatively enriched in both the CP and IP group.

Figure 3

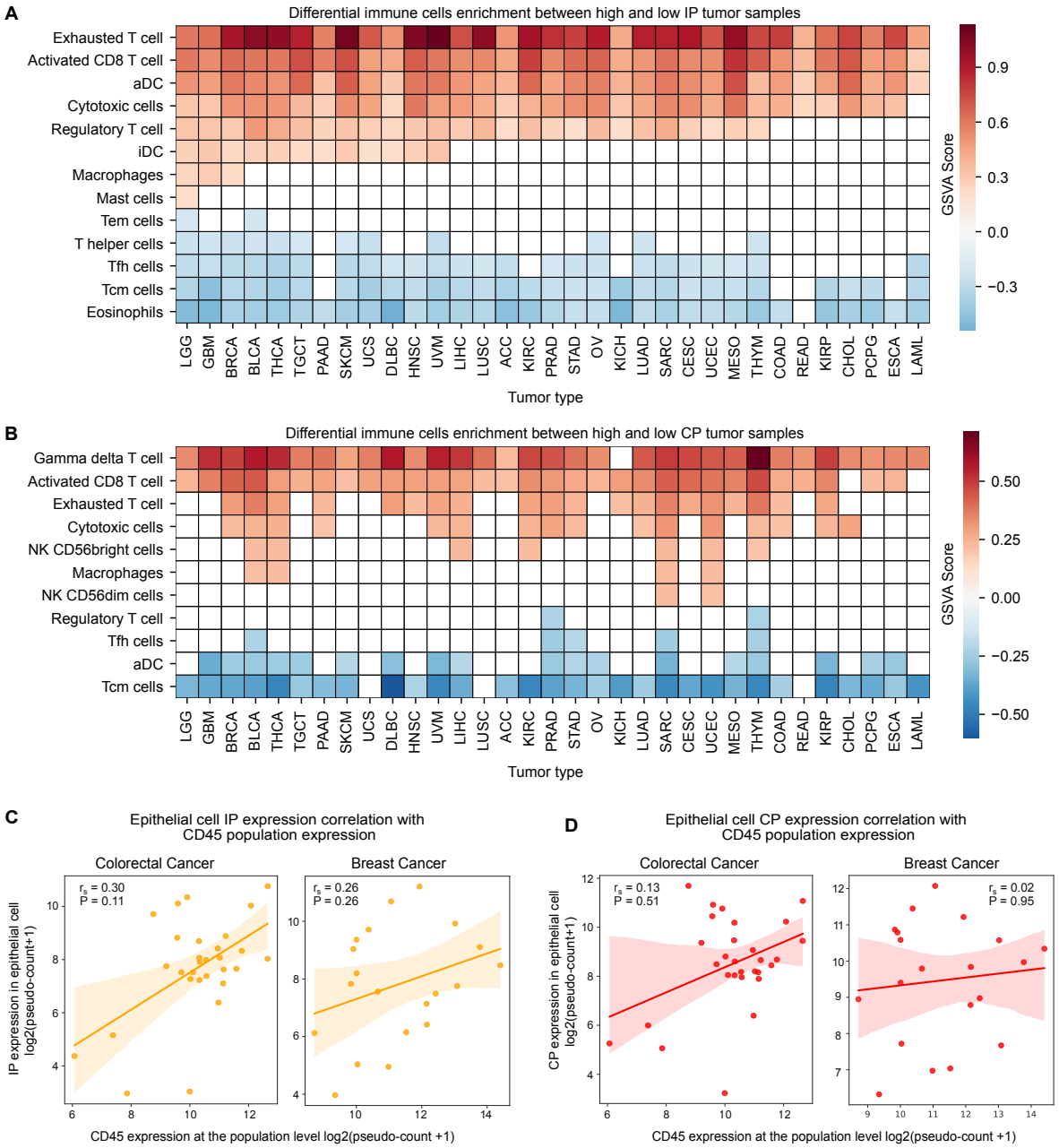

Figure 3: Immune cell enrichment associated with CP and IP expression

A. Heatmap represents the enrichment of different immune cell populations in tumours with high IP versus low IP expression group. The x-axis represents the tumour type and the y-axis represents the different immune cell type. The colour of each cell represents the GSVA score difference between the high versus low IP expression group. Only those tumour types and immune cells combinations with absolute GSVA score difference of 0.2 or greater and FDR adjusted p-value less than 0.1 were plotted here. The cells with white colour indicate no enrichment with respect to the above condition.
B. Same as **A**, but for the CP.
C. Spearman's rank correlation between CD45 gene expression and IP expression levels in epithelial cells (at the sample level) from colorectal and breast cancers.
D. Same as **C**, but for the CP.

Further, to investigate the effect of immune cells on the expression of proteasome in the tumour epithelial cells at a single-cell level, we compared proteasome expression with CD45 expression (see Methods). CD45 is a transmembrane glycoprotein expressed in all lymphocytes (26). The IP expression from tumour epithelial cells was highly correlated with CD45 expression from whole cell population in colorectal, breast, lung and oral cancer (Figure 3C, Supplementary Figure 2B). This can be attributed to the enrichment of cytotoxic immune cell infiltrations (as seen above); thus with an increase in the lymphocyte population we can see an increase in the IP expression also. CP also showed positive correlation with the increase in the lymphocyte population, however, the association strength was much weaker as compared to IP (Figure 3D, Supplementary Figure 2C). However, in kidney (renal cell) cancer, a negative correlation was observed for both IP and CP expression with the CD45 expression (Supplementary Figure 2B,C), which could be due to the lack of cytotoxic or interferon signalling in the TME.

Taken together, these results suggest that the presence of specific immune cells with cytotoxic activity correlates positively with IP expression in the tumour epithelial cells. This can potentially enhance the antigen presentation in tumour cells and attract more cytotoxic immune cells like a positive feedback mechanism.

High immunoproteasome expression is associated with inflammatory response and oxidative stress

Following the characterisation of TILs, we further asked which pathways are associated with the IP expression. For this, we performed differential pathway analysis of 50 MsigDb Hallmark gene-sets between high IP (top quartile) versus low IP samples (bottom quartile) for each tumour type, by using GSVA (see Methods, Supplementary Table 4). With the absolute enrichment score difference > 0.2 and FDR (q-value) < 0.01, we identified 7 upregulated and 6 downregulated pathways, recurrent in more than 40% of the tumour types (Figure 4A). The most frequently upregulated pathways are interferon-alpha (in 32 cancer types) and interferon-gamma (in 31 cancer types). Interferon signalling is known to induce IP formation in both immune and non-immune cells. Among all tumour types, DLBC and THYM did not show a significant increase in interferon-alpha and/or -gamma signalling, which

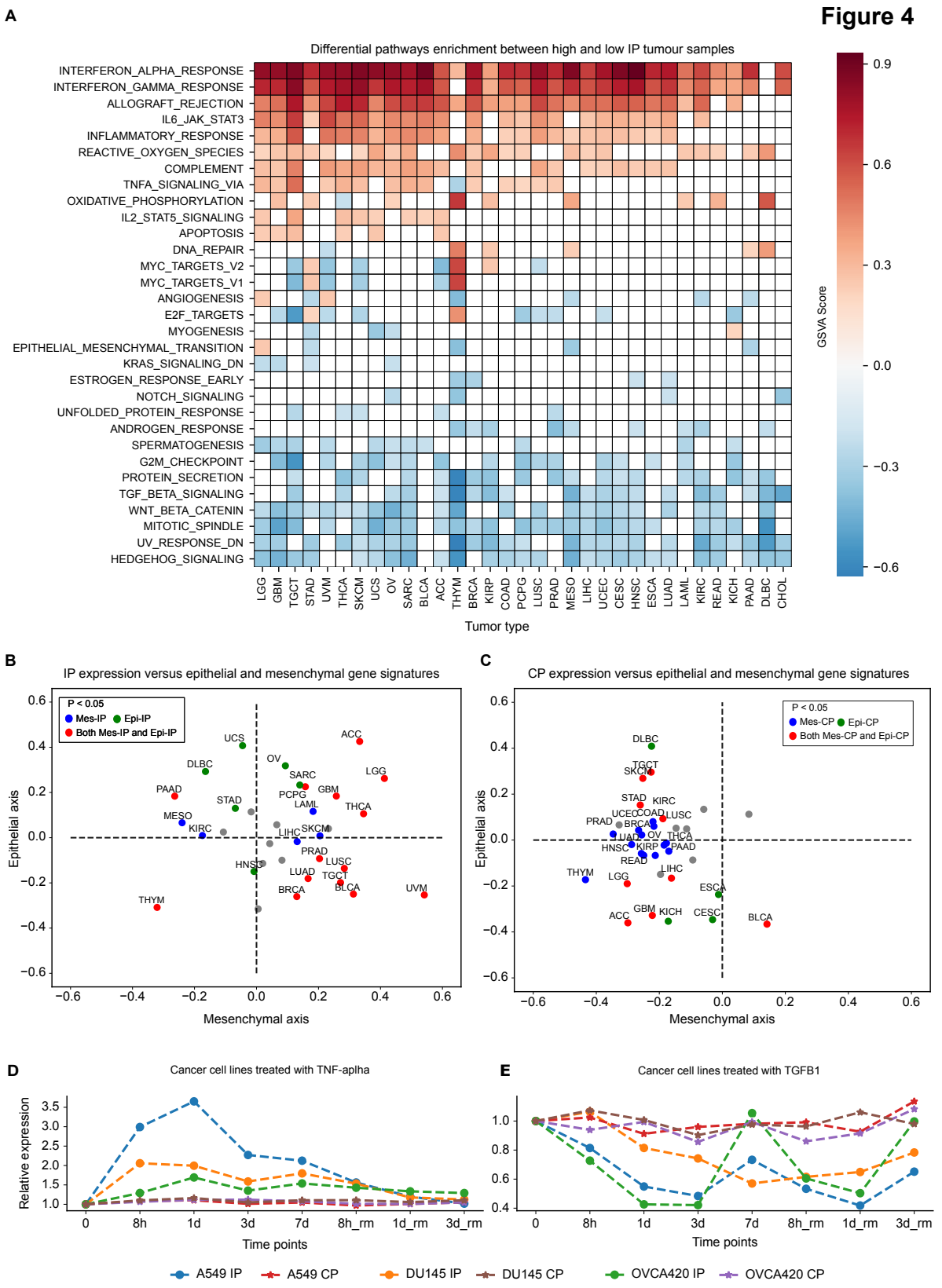

Figure 4: Pathways associated with proteasome expression

A. Differentially enrichment of cancer hallmark pathways between high and low IP expression sample groups. The x-axis represents the tumour type and the y-axis represents the different hallmark pathways (from MsigDB), and the colour of each cell represents the GSVA score difference between the high versus low IP expression group. Only those tumour types and pathway combinations with absolute GSVA score difference of 0.2 or greater and FDR adjusted p-values less than 0.01 were plotted here. The cells with white colour indicate no enrichment with respect to the above condition.

B. Correlation of IP expression with the epithelial specific (x-axis) and mesenchymal (y-axis) specific gene signatures. Each dot is a tumour type and the colour indicates whether the correlation with either the epithelial specific or mesenchymal specific gene signature, or both are significant (P<0.05) or non-significant (grey colour).
C. Same as **B**, but for the CP.
D-E. Relative expression changes in the IP and CP expression level in three different cancer cell lines (A549, lung; DU145, prostate; OVCA420, ovarian) treated with TNF alpha (**D**) and TGF-beta (**E**), respectively. The x-axis represents the different time points: untreated (0), under treatment (8h, 1 day, 3 days, 7 days) and withdrawal (rm) of treatment after 7 days of treatment (8h, 1 day and 3 days). The y-axis represents the relative expression change with respect to untreated condition (0). Each cancer cell line and proteasome (IP and CP) combination is highlighted with different lines.

could be attributed to the high basal level expression of the IP in these tumour types. The other pathways of upregulation in multiple cancer types are allograft rejection (n=28), IL-6/JAK/STAT3 signalling (n=24), inflammatory response (n=23), ROS pathway (n=22) and TNF-α signalling through NF-kB (n=14). The allograft rejection pathway has several overlapping genes with interferon signalling, which could explain their frequent upregulation. Upregulation of the ROS pathway with high IP expression is likely due to oxidative damage within the tumour cells and enrichment of inflammatory cells in the TME (27). TNF-α is a pro-inflammatory cytokine previously shown to induce the expression of IP subunits, either in synergy with IFN-γ or independently in a tissue-specific manner (28). However, none of these pathways (except ROS) were enriched in high CP tumour samples as compared to low CP samples (Supplementary Figure 3A).

Among the downregulated pathways with IP expression, the hedgehog (Hh) signalling (n=26), Mitotic spindle (n=25), UV response (n=25), Wnt-beta signalling (n=23), TGF-beta (TGF-β) signalling (n=20) and G2M checkpoint genes (n=17) were most frequent between the different cancer types (Figure 4A). The association of hedgehog signalling with low IP expression could be due to the suppression of CD8+T cell infiltration in the TME through the sonic hedgehog (SHH) mediated polarisation of tumour-associated macrophages (TAMs) (29). Similarly, the activation of Wnt-beta signalling has been shown to prevent the neoantigen-specific CD8+ T infiltration into the TME in NSCLC (30). TGF-β functions as an anti-inflammatory cytokine and it has been shown to downregulate the IP expression in NSCLC (13). Together, these results suggest that the IP expression in tumours is negatively

correlated with the immunosuppressive environment, which could be triggered by the tumour cell-intrinsic pathways and the types of immune cell infiltrating the TME.

A previous study has shown that the Epithelial-to-Mesenchymal Transition (EMT) negatively correlated with IP expression in NSCLC (13). However, our analysis found that the EMT pathway was downregulated in only four cancer types (Figure 4A). To further investigate this, we compared the expression of CP and IP with the epithelial-specific and mesenchymal-specific gene signatures (see Methods). The correlation of IP expression with mesenchymal signature was more distributed (Figure 4B): negative in certain tumours (HNSC, KIRC, PAAD, STAD and UCS) and positive in others (PRAD, GBM, THCA, LUSC, PCPG and BLCA). However, the CP expression was negatively correlated with mesenchymal-specific signatures (Figure 4C) and EMT (Supplementary Figure 3A) in multiple cancer types. Together, these results suggest that the EMT transition, particularly the upregulation of mesenchymal signature, downregulates the IP expression in a tumour-type specific manner as compared to CP.

Immunoproteasome expression is strongly associated with TNF-alpha and TGF-beta signalling

From the above analysis, we see certain pathways are consistent and strongly associated with up- and down-regulation of IP expression. However, it does not reveal how long it would take for these signalling cascades to induce or suppress the IP expression. To study this, we used the available time-course data of four different cancer cell lines (A549, lung; DU145, prostate; OVCA420, ovarian; MCF-7, breast) treated with TNF-alpha (positive regulatory of IP) and TGF-beta1 (negative regulatory of IP) (31). We observed that the treatment with TNF-alpha led to an increase in IP expression, with a roughly 2 to 3-fold increase at 8 hours or one-day post treatment, but not at the cost of CP expression level going down (Figure 4D). On the other hand, TGF-beta1 treatment led to a decrease in the expression, roughly two fold on day one or 3 days post-treatment, also without any difference in CP expression. This suggests that the induction and suppression rates of IP expression differ between TNF-alpha and TGF-beta1, respectively. However, in both cases, removal of cytokines brought the proteasome expression level closer to its pre-

treatment level (with some differences between the cell lines particularly for TGF-beta1). An exception to this is the MCF-7 cell line (Supplementary Figure 3B), which showed increased IP expression even after removal of TNF-alpha at 8 hours, and increase of IP expression with TGFB1 treatment (in contrast to other cancer cell lines as shown above).

Immunoproteasome gene expression is not correlated with somatic copy number changes

Next, we asked whether the proteasome (CP and IP genes) were targeted by somatic genetic alterations (mutations and/or copy number alterations) that favour the tumour cells for immune evasion. Surprisingly, we found that only a few samples (< 1%) harbour protein-affecting mutations (after removing hypermutator samples, see Methods, Supplementary Table 5). However, low level somatic copy number alterations were seen across different tumours (Supplementary Figure 4A). Deep deletion was observed in DLBC, albeit at a lower proportion of samples (~10%). However, a significant fraction of samples (above 50%) showed low-level amplification and deletions in both CP and IP across tumour types (KICH, UCS, OV and BRCA). Further, we asked whether the copy number alterations also lead to changes in gene expression. As expected, we observed a strong correlation between copy number changes and expression for each CP gene. However, for IP genes, we did not observe a strong association at the pan-cancer level (Supplementary Figure 4B) as well as at the individual tumour type level (Supplementary Figure 4C), suggesting that the induction of IP expression is likely dependent on the cytokine activity (as seen above).

Association of immunoproteasome expression with overall survival is influenced by immediate immune environment

We asked how IP expression influences patient survival using the TCGA cohort. Based on the Cox regression analysis, we found that the higher expression of IP was associated with better overall survival (FDR adjusted P<0.1) in six tumour types such as skin cutaneous melanoma (SKCM), cervical squamous cell carcinoma (CESC), breast invasive carcinoma (BRCA), bladder urothelial carcinoma (BLCA),

mesothelioma (MESO) and sarcoma (SARC). On the other hand, the expression of IP was associated with poor survival in kidney renal clear cell carcinoma (KIRC), acute myeloid leukaemia (LAML), brain lower grade glioma (LGG), and uveal melanoma (UVM) (Figure 5A).

Figure 5

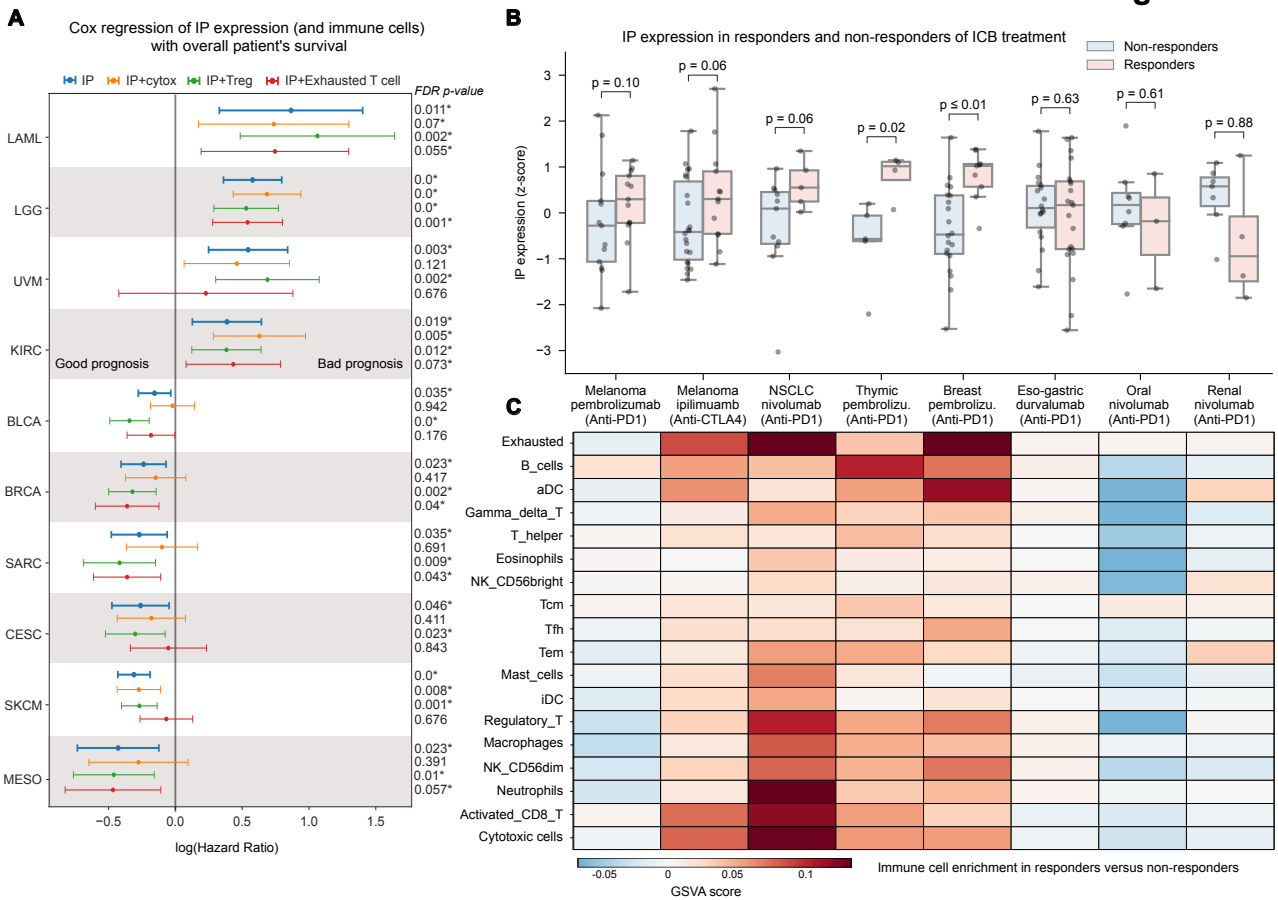

Figure 5: Association of IP expression with overall survival and response to immune checkpoint blockade (ICB) therapies

A. Cox proportional hazard ratio (HR) for IP expression alone and combined with three other confounders (regulatory T cell, Cytotoxic cells and exhaustive T cell) in 10 different tumour tissues from TCGA which showed significant association. The x-axis represents the log(Hazard Ratio) value, and the line represents the mean and 95% confidence interval. The colour of the line indicates the variables considered for the analysis. The P-value is calculated using Wald's test and subjected for multiple hypothesis testing using Benjamini-Hochberg method. The FDR corrected P-value is listed on the right side of the plot, and the asterisks(*) symbol indicates values less than 10% significance level.

B. The boxplot shows the average IP expression (represented as z-scores) in responders versus non-responders of ICB therapies in seven different tumour types from published studies. One-sided Mann-Whitney U test was used to compare whether the IP expression in responder was greater than non-responder, and the corresponding P-value reported at the top.

C. Heatmap representing the enrichment score difference of 18 different immune cells (based on its gene signature score) between responders and non-responders.

Given that the IP expression in bulk RNA-seq analysis has contributions from the infiltrating immune cells, we tried to adjust for their effects and other confounders such as age, gender, tumour stage and tumour mutational burden (TMB) of the samples independently and combined using multivariate Cox regression analysis (see Supplementary Table 6). This showed that the enrichment of different types of immune cells strongly influences the association of IP with survival in the above tumour types (as compared to other confounders). These immune cell types can be broadly classified into having anti- or pro-tumorigenic potential based on their functional properties. The anti-tumorigenic group includes cytotoxic cells such as CD8+ T cells, gamma delta T-cells and Natural Killer cells, whereas the pro-tumorigenic group includes regulatory T-cells (T-reg) and exhausted T-cells. When we adjusted for the enrichment of anti-tumorigenic (cytotoxic) immune cells, the hazard ratio (HR) increased and became non-significant (except for melanoma). This suggests the overwhelming role of cytotoxic immune cells (along with induction of IP expression in tumour cells) towards the better overall survival of patients.

On the other hand, the adjustment for the effect of regulatory T-cells, which are immunosuppressive in nature, the association of IP with better survival improved for the above tumour types, as well as for LGG which showed a bad prognosis with IP expression alone (Figure 5A). In the case of melanoma, the adjustment for neither cytotoxic nor T-reg impacted the association of IP with better survival, suggesting a cell-intrinsic or inherent higher expression of IP in this tumour type that favours better survival (17). Whereas, when we adjusted for exhausted T-cells (which have poor effector/tumour-eliminating function), the tumour types that showed poor survival with IP expression improved, and those tumour types with good survival (including melanoma) became worse, suggesting the presence of exhausted T-cell plays a different role in a tumour-type specific manner. With CP expression, we did not find any tumour type (except LGG) that showed good prognosis (Supplementary Figure 5A). Together, these results suggest that the IP expression is better associated with the overall survival of the patients, however, it is strongly influenced by the infiltrating immune cell types and their activity towards pro- or anti-tumorigenicity.

Association of immunoproteasome expression with response to immune checkpoint blockade therapies is tumour type specific

Next, we asked if the IP expression can be used as a predictor for immune checkpoint blockade (ICB) treatment response. To test this, we used data from eight publicly available studies across seven tumour types (Melanoma, Lung, Thymus, Eso-gastric, Breast, Oral and Renal) (see Methods, Supplementary Table 7). We compared the average IP expression (z-score) between the responders and non-responders on treatment with ICB (Figure 5B, Supplementary Table 8). In skin cutaneous melanoma, for both anti-PD1 (Pembrolizumab) and anti-CTLA4 (Ipilimumab), we see responders having a higher IP expression pre-treatment. This could be due to the enrichment of activated CD8+ T cells and cytotoxic cells in responders as compared to non-responders (Figure 5C) (32) (17). Similar trends can be seen in non-small cell lung cancer (Figure 5B), where patients with high IP expression respond better to the anti-PD1 treatment (Nivolumab). They also show high enrichment of neutrophils, activated CD8+ T cells and T-regs as compared to non-responders (Figure 5C). This enrichment profile matches with the hot immunophenotype of NSCLC cancer defined by Lizotte et al (33). A significant difference in the IP expression between responders and non-responders can be seen in thymic carcinoma (Figure 5B). Although the thymic epithelial tumours have the lowest TMB among adult cancers (34), the dysfunction in the T-cell development creates an autoreactive T-cell population. These autoreactive T-cells can recognise self-antigens and are known to increase IFN-gamma signalling which leads to the induction of IP genes and checkpoint receptors that can be beneficial for ICB response (35). Similarly, breast cancer patients (Figure 5B) also show high IP expression in responders as compared to non-responders of anti-PD1 therapy (Pembrolizumab). This is inline with the previous study (36) that showed enrichment of IFN-gamma, antigen presentation and checkpoint receptor gene sets in expanding T-cells with effector function on ICB treatment. Moreover, we see an overall enrichment of exhausted T-cells (37) (36) in cancer types which have a positive association of IP expression with ICB response (Figure 5C). This suggests that some of these exhausted T-cells might reactivate and gain effector function upon treatment (38).

However, we observed variability in the IP expression association with response to ICB therapy in other solid tumour types. In Eso-Gastric cancer, we did not see a difference in the IP expression and immune cell enrichment between the responders and non-responders of anti-PD1 treatment (Figure 5B). In oral and renal cancers, we observed lower IP expression in responders as compared to non-responders of anti-PD1 (Nivolumab) treatment. In the case of oral cancer, the downregulation of IP could be due to the enrichment of regulatory T-cells (T-regs) in the non-responders (Figure 5C). Whereas in renal cancers, we observed a relatively higher IP expression in non-responder despite their poor response to anti-PD1 therapy. This could be due to the low enrichment of cytotoxic immune cells in the TME (39) or other tumour-cell intrinsic factors (40). With CP expression, we did not find any significant difference between responder and responder across tumour types (Supplementary Figure 5B). Taken together, these results suggest that IP expression is strongly associated with response to ICB; however, in a tumour-type specific manner which can be due to the enrichment of tissue- and tumour-type specific immune infiltration patterns and their (tumour eliminating) effector function. Thus, IP expression combined with immune infiltration patterns could serve as a better predictor for ICB response in solid tumours.

Discussion

Though the immune checkpoint blockade (ICB) therapies are emerging anticancer therapy, the response rate is still variable within and across solid tumour types. To gain insights into this, recent studies have focused on the characterisation of genetic and molecular alterations at the tumour and immune cell levels, and whether these alterations can be used as biomarkers to predict response to ICB therapies (39,41,42). For example, the study by Kalaora et al., (17) showed that the IP gene expression can be used as a potential biomarker to predict prognosis and response to ICB therapy in skin melanoma. However, the extent of this in other solid tumours remains unclear. Thus, in this study, we explored the expression patterns of IP (in relation to CP) across multiple solid tumour types and identified cell-extrinsic and cell-intrinsic factors which influence the induction of IP expression and their association with the patient's overall survival and response to ICB therapies.

Although previous works have shown that the IP expression can be induced in non-immune cells upon exposure to pro-inflammatory signalling or stress conditions (1,4), it is not clear whether the induction of IP can affect the expression of CP. Here, we show that the expression of IP and CP were positively correlated in multiple tumour types (as compared to the normal tissues) (Figure 1A, 2F) and that the induction of IP does not hinder the CP expression (Figure 4D, E). We speculate that this could be due to potential co-regulation or cross-talk between the CP and IP gene expression in solid tumours (as previously shown in myeloma (43)). In addition, this observation raises the following questions: a) whether the CP expression is required for the switching of CP to IP assembly at the protein level; and b) whether the tumour cells require both CP and IP (or intermediate form) to modulate the antigen presentation (depending on the stress from the infiltrating immune cells). Future studies involving proteomics combined with epitope mapping could help to answer these questions and to understand the dynamics of active CP and IP complexes in shaping the antigen presentation and immunogenicity in tumour cells.

In most of the solid tumour types, the IP expression was positively correlated with the cytotoxic immune cell infiltrations and upregulation of genes involved in interferon signalling pathways and reactive oxygen species (Figure 3 and 4), suggesting that the induction of IP is influenced by both cell-extrinsic and cell-intrinsic pathways. However, within the tumour tissue, the expression of IP was highly variable among tumour epithelial cells: only a subset of cells expressing high IP, in particular, those at the tumour border than tumour core regions (Figure 2 E and G). Recent studies have shown that the spatial enrichment of cytotoxic immune cells plays a vital role in the interferon signalling and response to ICB therapies (41,44). Based on this, we speculate that the variation observed in IP expression among tumour cells may be due to the differential exposure of tumour cells to the cytotoxic immune cells and interferon signalling. However, future studies involving the spatial-temporal analysis of immune cell infiltration patterns and cell-cell interactions across different cancer types could reveal the complex interaction between the tumour cells and immune cells, and their impact on induction of IP expression.

Finally, we showed that the association of IP expression with overall survival and response to ICB therapies is tumour type specific (Figure 5). In certain tumour types, the IP expression was associated with better prognosis and response to ICB therapies. However, this association was highly influenced by the enrichment of cytotoxic immune cell infiltration in the tumour microenvironment, except for skin melanoma (as shown previously (17)). In some tumour types, we did not find any association. Whereas, in a few tumour types, we observed that the IP expression was associated with poor prognosis and non-response to ICB therapies, and this is likely due to the enrichment of immunosuppressive immune cells (like Tregs) or low enrichment of cytotoxic immune cells. In sum, our study reveals that the expression of IP combined with immune cell infiltration scores can be used as a potential marker to predict prognosis and response to ICB therapies in solid tumours. However, further studies with more samples and cancer types with response data of ICB therapies are required to validate these findings and also to explore whether the IP expression has any oncogenic roles in these tumours besides their expected role in the protein degradation.

Materials and Methods

TCGA and GTEx data processing

Somatic mutations (MC3), copy number alterations, tumour purity and gene expression (RSEM gene normalised) data for 9,491 tumours across 33 different tumour types were obtained from the TCGA pan-can atlas study (https://gdc.cancer.gov/about-data/publications/pancanatlas). The gene expression (RSEM gene normalised) data from normal tissues of 6,125 GTEx samples (across 37 tissue types) was obtained from the UCSC Xena browser (45). The expression (RSEM) values were log2 transformed (after adding 1) and then computed an average expression value for CP (mean of PSMB5, PSMB6, PSMB7 genes) and IP (mean of PSMB8, PSMB9, PSMB10 genes) at each individual sample level (Figure 1A,B). The relationship between the average expression of CP and IP was estimated using Spearman's rank correlation approach. The matched normal tissue (from GTEx) for

each tumour type shown in Figure 1C-E was selected based on the information given in UCSC Xena browser. The sample details were given in Supplementary Table 1.

Single-cell data processing

We have collated single-cell gene expression data from previous studies covering nine tumour types: Kidney, Pancreas, Prostate, Colorectal, Lung, Breast, Liver, Ovarian and Oral (see Supplementary Table 2). The number of samples and single-cell counts under each cohort are listed in Supplementary Table 2. For studies which provided raw UMI counts, the counts were normalised at cell level by the total counts over all genes using scanpy (46) (sc.pp.normalize_total function with target_sum = 1e4). Further, the values were log2 transformed (after adding 1) and then computed the average expression value for CP (mean of PSMB5, PSMB6 and PSMB7 genes) and IP (mean of PSMB8, PSMB9, and PSMB10) at each cell. To calculate the proportion of cells expressing IP and CP under different cell types (tumour epithelial cells, T-cells and B-cells) shown in Figure 2G, we selected tumour types which have those three cell types available and calculated the fraction of cells with average proteasome expression (IP or CP) greater than the median average proteasome expression value (IP or CP) in the respective cell types. Similarly, for the sample level comparison (shown in Figures 2F and 3C), we considered cells with average proteasome expression values above the median value in the respective cell type and calculated the sum of the average proteasome expression values across all cells within that sample (represented as pseudo-counts). Spearman's rank correlation analysis was used to compare proteasome expression at the sample level in Figures 2F and 3C.

Enrichment analysis of immune cells and pathways

We performed a single sample gene set enrichment analysis (ssGSVA) using R package GSVA (47) to quantify the infiltration level of 18 different immune cells (Cytotoxic cells, Regulatory T cell, Gamma delta T cell, Activated CD8 T cell, iDC, aDC, Tfh cells, Tem Cells, Tcm Cells, T helper cells, Neutrophils, NK CD56dim cells, NK CD56 bright cells, Mast cells, Macrophages, Eosinophils, B cells and Exhausted T-cells) by using their respective gene signatures from Tamborero et al., (48), except

for the exhausted T-cell for which we considered three genes (LAG3, HAVCR2, PDCD1) from (36,49). The 50 different hallmark pathways were obtained from MsigDB (50). The differential pathways and immune cell enrichment between high (>75th percentile) and low proteasome (<25th percentile) of IP or CP groups were carried out through the GSVA pipeline (47). The absolute GSAV score of 0.2 or greater with FDR corrected P-value < 0.1 was considered significant. The gene signatures associated with epithelial-specific and mesenchymal specific were obtained from Tan et al (51). These gene lists were given in Supplementary Table 9.

Cancer cell lines data analysis

The time-course data of four cancer cell lines (A549, lung; DU145, prostate; OVCA420, ovarian and MCF-7, breast) treated with TNF alpha and TFGB1 was obtained from the Gene Expression Omnibus under the accession GSE147405 (31). This dataset consists of gene expression values (at the single cell level) for 5 different time points (8h, 1 day, 3 days, and 7 days) with treatment and 3 additional time points (8h, 1 day and 3 day) without treatment, following the last treatment point (7 days). The count values were normalised at each cell level by the total counts over all genes. For each PSMB gene, we first computed the average value across the single cells under each condition and time point. Then, the average expression value of CP (mean of PSMB5, PSMB6 and PSMB7) and IP (mean of PSMB8, PSMB9, and PSMB10) was computed for each condition and time point. The relative change in the expression of IP and CP has been computed with respect to the average expression level at the initial time point (t=0).

Genetic alterations in proteasome genes

To check if the CP and IP genes were affected by somatic alterations, we considered non-synonymous mutations and copy number alterations (amplification/deletions) in the six PSMB genes. For the mutation analysis, we removed hypermutator samples (>10 mutations/MB) (52). Further, we computed the fraction of samples having the protein affecting mutation in the IP and CP genes. Similarly, we computed the fraction of samples having copy number alteration (amplified or deleted) in each of these genes in all of 33 tumour types.

Cox proportional hazard ratio and survival analysis

To assess the association of IP expression with the survival of the patients, we collected the clinical status of the samples from the TCGA pan-can atlas study. We performed univariate and multivariate Cox's regression analysis by taking IP and its different confounders as covariates (cytotoxic infiltration level, regulatory T cell infiltration level, Exhaustive T cell expression level, age, sex, tumour stage, tumour mutational burden) independently and combined to assess the prognostic association across tumour tissues, by using lifeline package written in Python (https://lifelines.readthedocs.io/). The p-values computed using Wald's test were subjected to multiple hypothesis testing corrections using the Benjamini-Hochberg approach (see Supplementary Table 6). Prior to that, the tumour types (THYM, TGCT, PCPG, DLBC, THCA and KICH) which were not recommended for overall survival analysis or with low number of cases were removed according to the Liu et al., study (53).

Immunoproteasome association with ICB response

Data from eight publicly available studies across seven tumour types (Melanoma, Lung, Thymic carcinoma, Breast, Oral and Renal) was used to investigate the IP expression association with ICB response (Supplementary Table 7). The average proteasome score was computed as the average of log2 transformed values of PSMB5, PSMB6 and PSMB7 for CP and PSMB8, PSMB9, and PSMB10 for IP. To compare the trends across multiple studies, the average scores were transformed into a z-score for each tumour type/dataset (Supplementary Table 8). Further, a single sample scoring method (54) was used to calculate the enrichment score of 18 immune signatures and then performed differential enrichment analysis between responders and non-responders using the GSVA pipeline.

Acknowledgements

We thank Dr Dimple Notani and members of RS lab for feedback and suggestions. The results shown here are in part based upon data generated by the TCGA Research Network: https://www.cancer.gov/tcga. We acknowledge support of the Department of Atomic Energy, Government of India, under Project Identification No. RTI 4006 and intramural funds from NCBS-TIFR.

References

1. Kimura H, Caturegli P, Takahashi M, Suzuki K. New Insights into the Function of the Immunoproteasome in Immune and Nonimmune Cells. J Immunol Res. 2015;2015:541984.

2. Morozov AV, Karpov VL. Proteasomes and Several Aspects of Their Heterogeneity Relevant to Cancer. Front Oncol. 2019;9:761.

3. Murata S, Takahama Y, Kasahara M, Tanaka K. The immunoproteasome and thymoproteasome: functions, evolution and human disease. Nat Immunol. 2018;19:923–31.

4. Johnston-Carey HK, Pomatto LCD, Davies KJA. The Immunoproteasome in oxidative stress, aging, and disease. Crit Rev Biochem Mol Biol. 2015;51:268–81.

5. Eskandari SK, Seelen MAJ, Lin G, Azzi JR. The immunoproteasome: An old player with a novel and emerging role in alloimmunity. Am J Transplant. 2017;17:3033–9.

6. Heink S, Ludwig D, Kloetzel P-M, Krüger E. IFN-γ-induced immune adaptation of the proteasome system is an accelerated and transient response. Proceedings of the National Academy of Sciences. 2005. page 9241–6.

7. Griffin TA, Nandi D, Cruz M, Fehling HJ, Van Kaer L, Monaco JJ, et al. Immunoproteasome Assembly: Cooperative Incorporation of Interferon γ (IFN-γ)–inducible Subunits. Journal of Experimental Medicine. 1998. page 97–104.

8. Specht G, Roetschke HP, Mansurkhodzhaev A, Henklein P, Textoris-Taube K, Urlaub H, et al. Large database for the analysis and prediction of spliced and non-spliced peptide generation by proteasomes. Sci Data. 2020;7:146.

9. Winter MB, La Greca F, Arastu-Kapur S, Caiazza F, Cimermancic P, Buchholz TJ, et al. Immunoproteasome functions explained by divergence in cleavage specificity and regulation. Elife. 2017;6.

10. Van Kaer L, Ashton-Rickardt PG, Eichelberger M, Gaczynska M, Nagashima K, Rock KL, et al. Altered peptidase and viral-specific T cell response in LMP2 mutant mice. Immunity. 1994;1:533–41.

11. van den Eshof BL, Medfai L, Nolfi E, Wawrzyniuk M, Sijts AJA. The Function of Immunoproteasomes—An Immunologists' Perspective Cells. 2021 Dec; 10(12): 3360.

12. Kalim KW, Basler M, Kirk CJ, Groettrup M. Immunoproteasome subunit LMP7 deficiency and inhibition suppresses Th1 and Th17 but enhances regulatory T cell differentiation. J Immunol 2012;189(8):4182-93.

13. Tripathi SC, Peters HL, Taguchi A, Katayama H, Wang H, Momin A, et al. Immunoproteasome deficiency is a feature of non-small cell lung cancer with a mesenchymal phenotype and is associated with a poor outcome. Proc Natl Acad Sci U S A. 2016;113:E1555–64.

14. Niewerth D, Kaspers GJL, Jansen G, van Meerloo J, Zweegman S, Jenkins G, et al. Proteasome subunit expression analysis and chemosensitivity in relapsed paediatric acute leukaemia patients receiving bortezomib-containing chemotherapy. J Hematol Oncol. 2016;9:82.

15. Tubío-Santamaría N, Ebstein F, Heidel FH, Krüger E. Immunoproteasome Function in Normal and Malignant Hematopoiesis. Cells. 2021 10(7): 1577.

16. Tripathi SC, Vedpathak D, Ostrin EJ. The Functional and Mechanistic Roles of Immunoproteasome Subunits in Cancer. Cells. 2021; 10(12): 3587.

17. Kalaora S, Lee JS, Barnea E, Levy R, Greenberg P, Alon M, et al. Immunoproteasome expression is associated with better prognosis and response to checkpoint therapies in melanoma. Nat Commun. 2020;11:896.

18. Rouette A, Trofimov A, Haberl D, Boucher G, Lavallée V-P, D'Angelo G, et al. Expression of

immunoproteasome genes is regulated by cell-intrinsic and –extrinsic factors in human cancers. Scientific Reports. 2016; 6: 34019.

19. Hwang S, Kwon A-Y, Jeong J-Y, Kim S, Kang H, Park J, et al. Immune gene signatures for predicting durable clinical benefit of anti-PD-1 immunotherapy in patients with non-small cell lung cancer. Sci Rep. 2020;10:643.

20. Lee HO, Hong Y, Etlioglu HE, Cho YB, Pomella V, den Bosch B V, et al. Lineage-dependent gene expression programs influence the immune landscape of colorectal cancer. Nat Genet 2020. 52(6):594-603

21. Yi JS, Cox MA, Zajac AJ. T-cell exhaustion: characteristics, causes and conversion. Immunology. 2010;129:474.

22. Togashi Y, Shitara K, Nishikawa H. Regulatory T cells in cancer immunosuppression — implications for anticancer therapy. Nat Rev Clin Oncol. 2019;16:356–71.

23. Gardner A, de Mingo Pulido Á, Ruffell B. Dendritic Cells and Their Role in Immunotherapy. Front Immunol 2020; 11: 924.

24. Dudek AM, Martin S, Garg AD, Agostinis P. Immature, Semi-Mature, and Fully Mature Dendritic Cells: Toward a DC-Cancer Cells Interface That Augments Anticancer Immunity. Front Immunol. 2013; 4: 438.

25. Nielsen MM, Witherden DA, Havran WL. γδ T cells in homeostasis and host defence of epithelial barrier tissues. Nat Rev Immunol. 2017;17:733.

26. Leister H, Krause FF, Mahdavi R, Steinhoff U, Visekruna A. The Role of Immunoproteasomes in Tumor-Immune Cell Interactions in Melanoma and Colon Cancer. Arch Immunol Ther Exp . Springer; 2022;70:1–7.

27. Aggarwal V, Tuli HS, Varol A, Thakral F, Yerer MB, Sak K, et al. Role of Reactive Oxygen Species in Cancer Progression: Molecular Mechanisms and Recent Advancements. Biomolecules. 2019 9(11):735.

28. Angeles A, Fung G, Luo H. Immune and non-immune functions of the immunoproteasome. Front Biosci . 2012;17:1904–16.

29. Petty AJ, Li A, Wang X, Dai R, Heyman B, Hsu D, et al. Hedgehog signaling promotes tumor-associated macrophage polarization to suppress intratumoral CD8+ T cell recruitment. J Clin Invest. 2019;129:5151–62.

30. Takeuchi Y, Tanegashima T, Sato E, Irie T, Sai A, Itahashi K, et al. Highly immunogenic cancer cells require activation of the WNT pathway for immunological escape. Sci Immunol. 2021;6:eabc6424.

31. Cook DP, Vanderhyden BC. Context specificity of the EMT transcriptional response. Nat Commun. 2020;11:2142.

32. Ralli M, Botticelli A, Visconti IC, Angeletti D, Fiore M, Marchetti P, et al. Immunotherapy in the Treatment of Metastatic Melanoma: Current Knowledge and Future Directions. Journal of Immunology Research 2020:9235638.

33. Lizotte PH, Ivanova EV, Awad MM, Jones RE, Keogh L, Liu H, et al. Multiparametric profiling of non-small-cell lung cancers reveals distinct immunophenotypes. JCI insight 2016 Sep 8;1(14):e89014

34. Radovich M, Pickering CR, Felau I, Ha G, Zhang H, Jo H, et al. The integrated genomic landscape of thymic epithelial tumors. Cancer Cell. 2018;33:244.

35. Tateo V, Manuzzi L, De Giglio A, Parisi C, Lamberti G, Campana D, et al. Immunobiology of Thymic Epithelial Tumors: Implications for Immunotherapy with Immune Checkpoint Inhibitors. Int J Mol Sci 2020 Dec; 21(23): 9056.

36. Bassez A, Vos H, Van Dyck L, Floris G, Arijs I, Desmedt C, et al. A single-cell map of intratumoral

changes during anti-PD1 treatment of patients with breast cancer. Nat Med. 2021;27:820–32.

37. Defining T Cell States Associated with Response to Checkpoint Immunotherapy in Melanoma. Cell. 2018;175:998–1013.e20.

38. Blank CU, Haining WN, Held W, Hogan PG, Kallies A, Lugli E, et al. Defining “T cell exhaustion.” Nat Rev Immunol. 2019;19:665–74.

39. Au L, Hatipoglu E, Robert de Massy M, Litchfield K, Beattie G, Rowan A, et al. Determinants of anti-PD-1 response and resistance in clear cell renal cell carcinoma. Cancer Cell. 2021;39:1497–518.e11.

40. Ascierto ML, McMiller TL, Berger AE, Danilova L, Anders RA, Netto GJ, et al. The Intratumoral Balance between Metabolic and Immunologic Gene Expression Is Associated with Anti-PD-1 Response in Patients with Renal Cell Carcinoma. Cancer Immunol Res. 2016;4:726–33.

41. Hammerl D, Martens JWM, Timmermans M, Smid M, Trapman-Jansen AM, Foekens R, et al. Spatial immunophenotypes predict response to anti-PD1 treatment and capture distinct paths of T cell evasion in triple negative breast cancer. Nat Commun. 2021;12:5668.

42. Kourtis N, Wang Q, Wang B, Oswald E, Adler C, Cherravuru S, et al. A single-cell map of dynamic chromatin landscapes of immune cells in renal cell carcinoma. Nat Cancer. 2022;3:885–98.

43. Bhat P, Leggatt G, Waterhouse N, Frazer IH. Interferon-γ derived from cytotoxic lymphocytes directly enhances their motility and cytotoxicity. Cell Death Dis. 2017;8:e2836–e2836.

44. Barkley D, Moncada R, Pour M, Liberman DA, Dryg I, Werba G, et al. Cancer cell states recur across tumor types and form specific interactions with the tumor microenvironment. Nat Genet. 2022;54:1192–201.

45. Goldman MJ, Craft B, Hastie M, Repečka K, McDade F, Kamath A, et al. Visualizing and interpreting cancer genomics data via the Xena platform. Nat Biotechnol. 2020;38:675–8.

46. Wolf FA, Angerer P, Theis FJ. SCANPY: large-scale single-cell gene expression data analysis. Genome Biol. 2018;19:15.

47. Hänzelmann S, Castelo R, Guinney J. GSVA: gene set variation analysis for microarray and RNA-seq data. BMC Bioinformatics. 2013;14:7.

48. Tamborero D, Rubio-Perez C, Muiños F, Sabarinathan R, Piulats JM, Muntasell A, et al. A Pan-cancer Landscape of Interactions between Solid Tumors and Infiltrating Immune Cell Populations. Clin Cancer Res. 2018;24:3717–28.

49. van der Leun AM, Thommen DS, Schumacher TN. CD8+ T cell states in human cancer: insights from single-cell analysis. Nat Rev Cancer. 2020;20:218.

50. Liberzon A, Birger C, Thorvaldsdóttir H, Ghandi M, Mesirov JP, Tamayo P. The Molecular Signatures Database (MSigDB) hallmark gene set collection. Cell Syst. 2015;1:417–25.

51. Tan TZ, Miow QH, Miki Y, Noda T, Mori S, Huang RY-J, et al. Epithelial-mesenchymal transition spectrum quantification and its efficacy in deciphering survival and drug responses of cancer patients. EMBO Mol Med. 2014;6:1279–93.

52. Martincorena I, Raine KM, Gerstung M, Dawson KJ, Haase K, Van Loo P, et al. Universal Patterns of Selection in Cancer and Somatic Tissues. Cell. 2017;171:1029–41.e21.

53. Liu J, Lichtenberg T, Hoadley KA, Poisson LM, Lazar AJ, Cherniack AD, et al. An Integrated TCGA Pan-Cancer Clinical Data Resource to Drive High-Quality Survival Outcome Analytics. Cell. 2018;173:400–16.e11.

54. Foroutan M, Bhuva DD, Lyu R, Horan K, Cursons J, Davis MJ. Single sample scoring of molecular phenotypes. BMC Bioinformatics. 2018;19:1–10.

Supplementary Figures:

Supplementary Figure 1

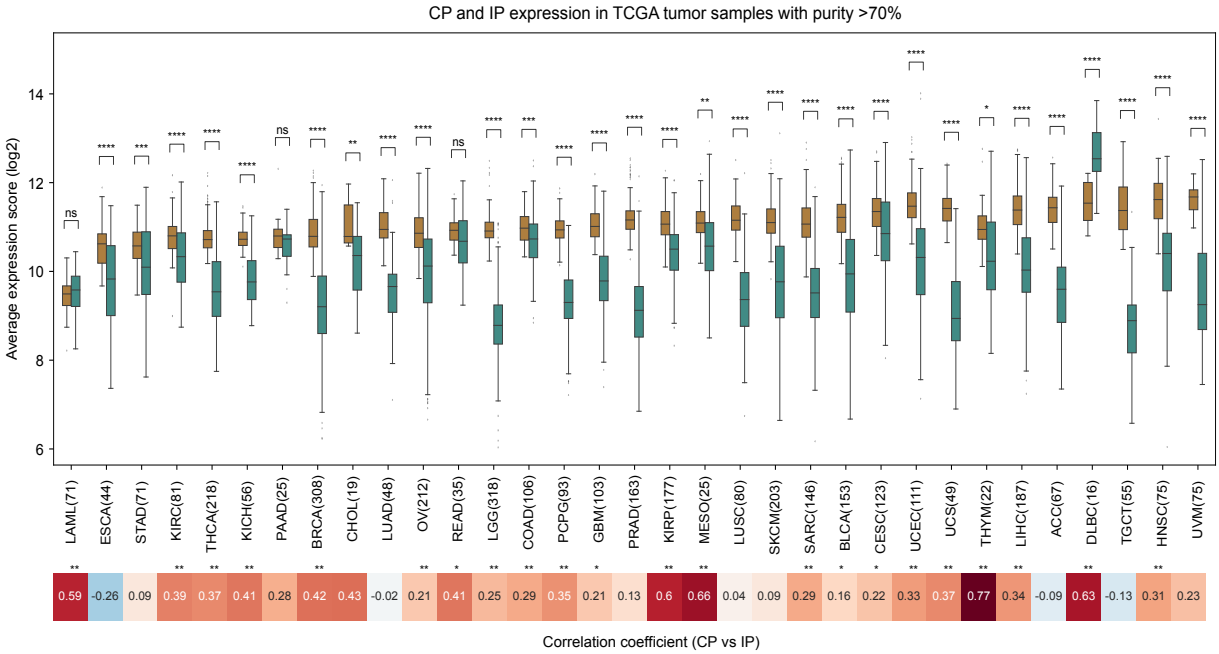

Supplementary Figure 1: Comparison of CP and IP expression in tumours with high purity (>70%)

The boxplot represents the distribution of gene expression levels of constitutive proteasome (CP) and immunoproteasome (IP) across multiple tumour tissues from TCGA. The x-axis represents the tumour tissues (and the number of samples with tumour purity >70%) and the y-axis represents the log2 average expression (RSEM+1) of core genes of CP (PSMB5, PSMB6 and PSMB7) and IP (PSMB8, PSMB9 and PSMB10) (see Methods). The P-values were computed using Mann-Whitney U test (two-sided) and and the significance level was represented as * p<0.05,** p<0.01 or ns - non-significant (P>=0.05). The heatmap at the bottom represents the Spearman's rank correlation between CP and IP expression and the asterisk symbol on the top indicates the P-value (as mentioned above).

Supplementary Figure 2

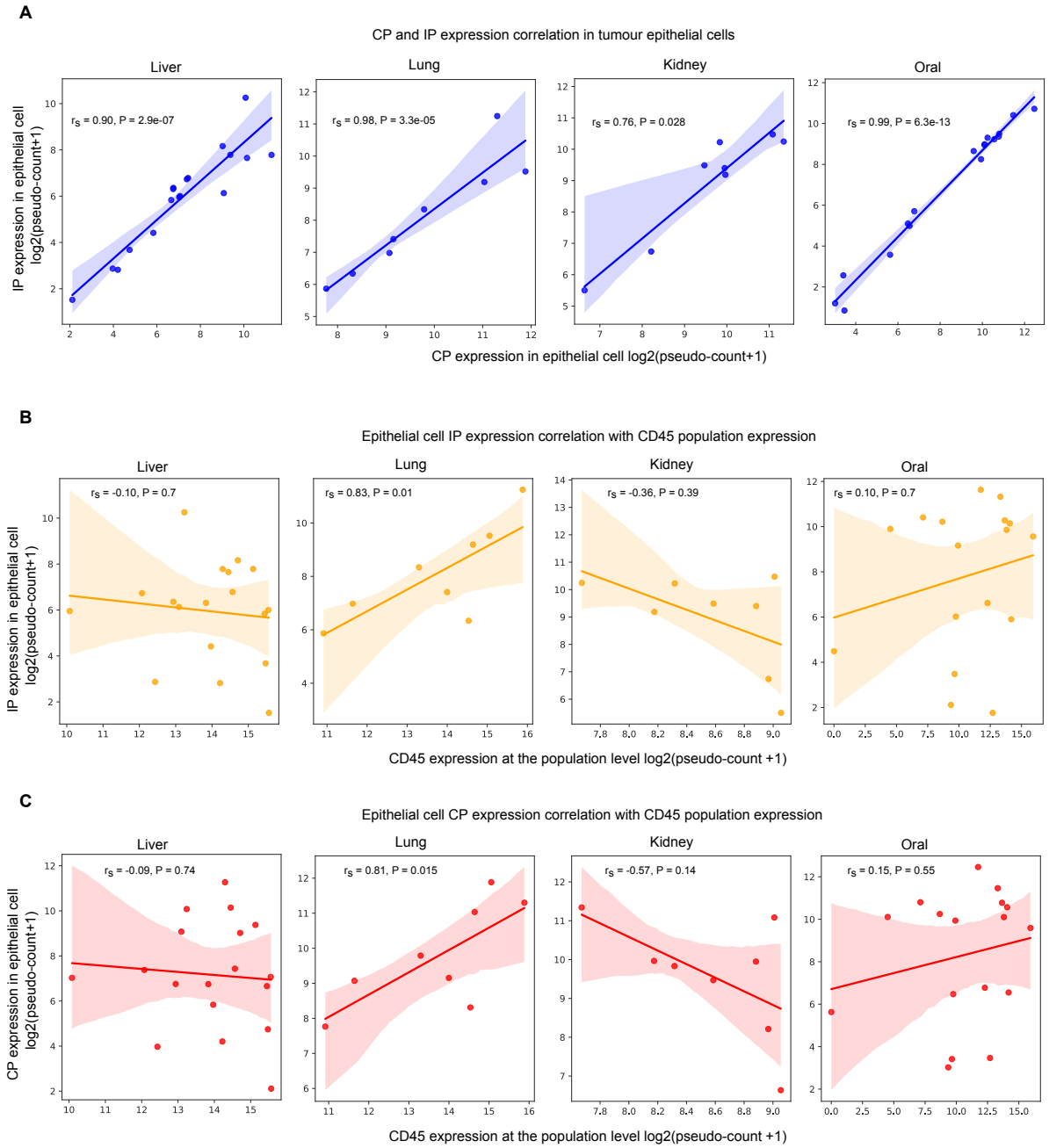

Supplementary Figure 2: Single-cell analysis of CP and IP expression across tumours

A. Spearman's rank correlation between the average expression of CP and IP genes (from tumour epithelial cell population) in liver, lung, kidney and oral cancers. Each dot represents a sample and the values on the x- and y-axis represent the proteasome expression as pseud-count (i.e., average expression of CP or IP genes across all cells within the sample). **B**. Spearman's rank correlation between CD45 gene expression (from all cells) and IP expression from epithelial cells (at the sample level) in liver, lung, kidney and oral cancers. **C**. Same as B, but for CP.

Supplementary Figure 3

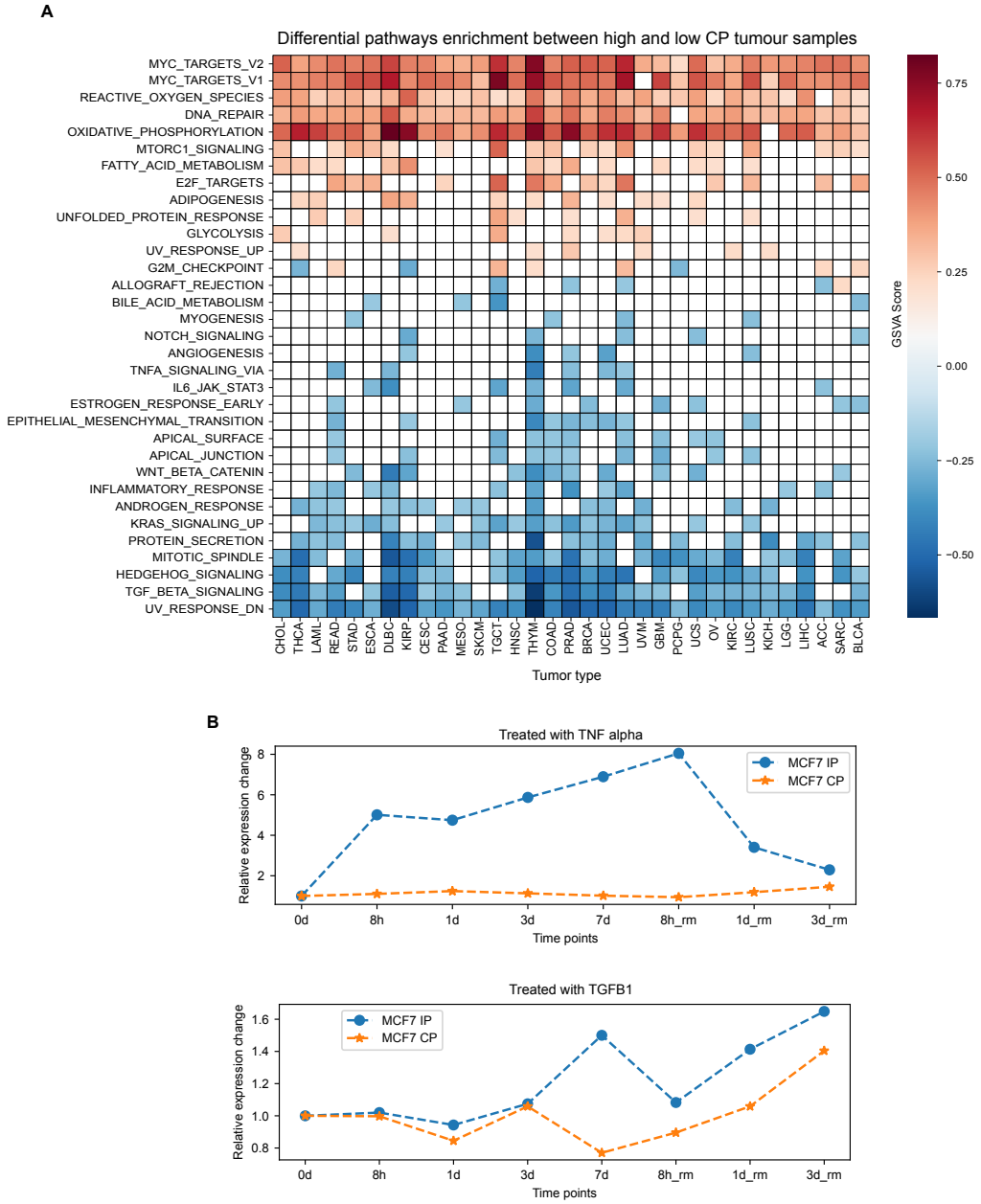

Supplementary Figure 3: Differential pathway enrichment between high and low CP tumour samples

A. Differentially enrichment of cancer hallmark pathways between high and low CP expression sample groups. The x-axis represents the tumour type and the y-axis represents the different hallmark pathways (from MsigDB), and the colour of each cell represents the GSVA score difference between the high versus low IP expression group. Only those tumour types and pathway combinations with absolute GSVA score difference of 0.2 or greater and FDR adjusted p-values less than 0.05 were plotted here. The cells with white colour indicate no enrichment with respect to the above condition.

B. Relative expression changes in the IP and CP expression level in MCF-7 breast cancer cell line. The x-axis represents the different time points: untreated (0), under treatment (8h, 1 day, 3 days, 7 days) and withdrawal (rm) of treatment after 7 days of treatment (8h, 1 day and 3 days). The y-axis represents the relative expression change with respect to untreated condition (0).

Supplementary Figure 4

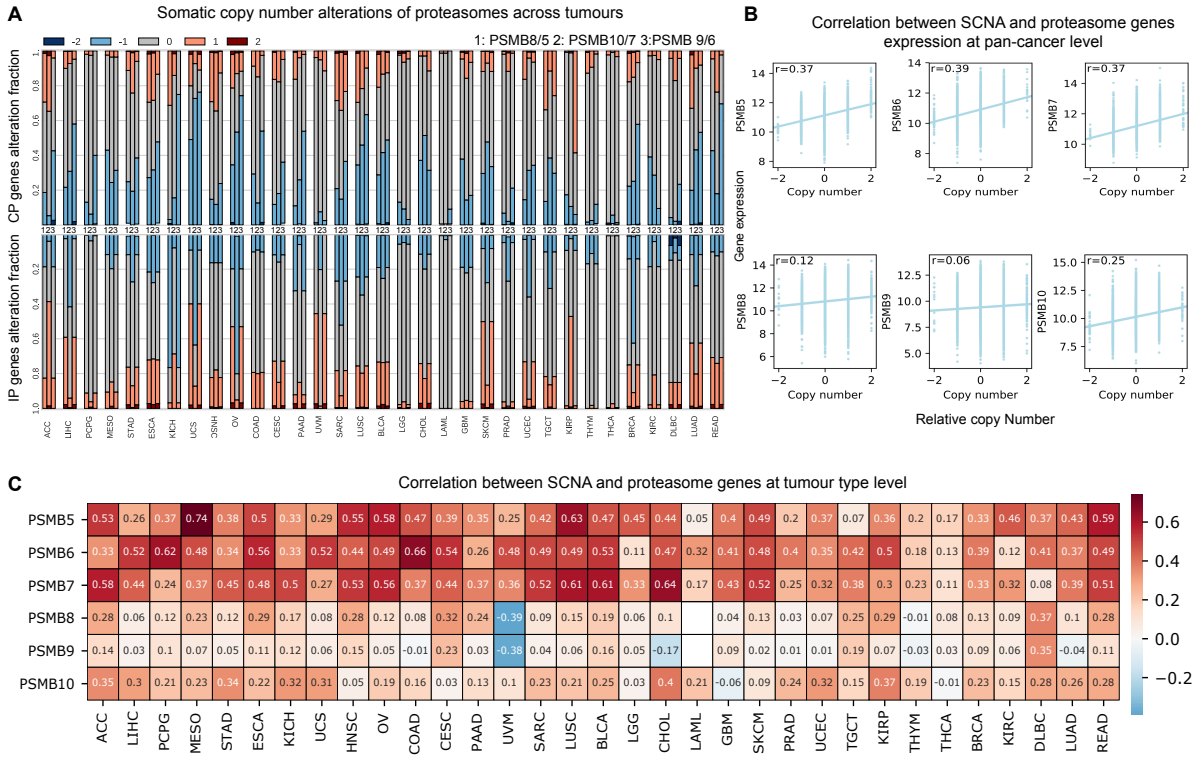

Supplementary Figure 4: Somatic copy number alterations in proteasome genes and their correlation with gene expression

A. Proportion of tumour samples having somatic copy number alteration in CP (PSMB5, PSMB6, PSMB7) and IP(PSMB8, PSMB9, PSMB10) genes. The stacked bar plot represents the fraction of samples with no somatic copy number alterations (zero), deletion (-1), deep deletion (-2), amplification (1) and high level amplification (2) under each tumour type. The top row is for CP genes and the columns 1, 2 and 3 represent PSMB5, 7 and 6; and the bottom row is for IP genes and the columns 1, 2 and 3 represent PSMB8, 10, 9.

B-C.Spearman's rank correlation between somatic copy number alteration and CP and IP genes individually at the pan-cancer level (**B**), and at the individual tumour type level (**C**).

Supplementary Figure 5

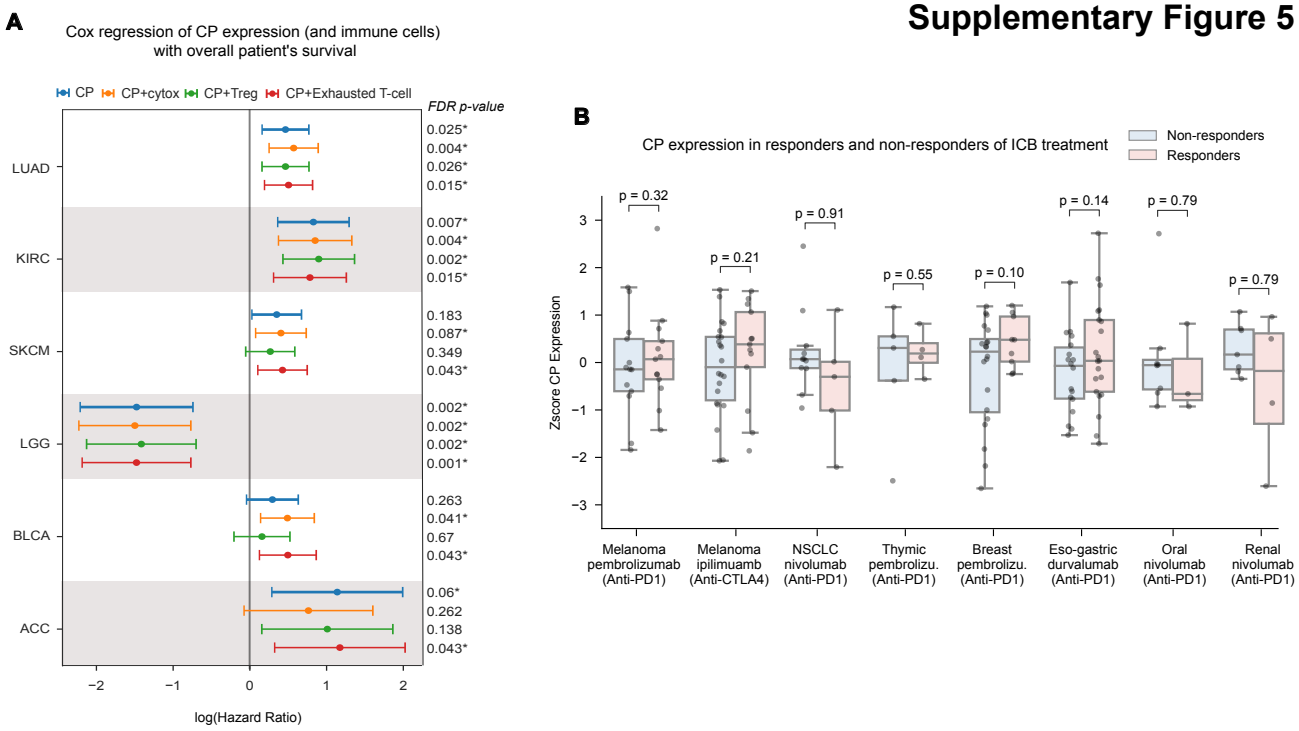

Supplementary Figure 5: Association of IP expression with overall survival and response to immune checkpoint blockade (ICB) therapies

A. Cox proportional hazard ratio (HR) for CP expression alone and combined with three other confounders (regulatory T cell, Cytotoxic cells and exhaustive T cell) in six different tumour tissues from TCGA which showed significant association. The x-axis represents the log(HR) value, and the line represents the mean and 95% confidence interval. The colour of the line indicates the variables considered for the analysis. The P-value is calculated using Wald's test and subjected for multiple hypothesis testing using Benjamini-Hochberg method. The FDR corrected P-value is listed on the right side of the plot, and the asterisk(*) symbol indicates values less than 10% significance level.

B. The boxplot shows the average CP expression (represented as z-scores) in responders versus non-responders of ICB therapies in seven different tumour types from published studies. One-sided Mann-Whitney U test was used to compare whether the IP expression in responder was greater than non-responder, and the corresponding P-value reported at the top.

Supplementary Tables:

Supplementary Table 1: Gene expression values of IP and CP genes in TCGA and GTEx samples. **A:** Proteasome gene expression level in TCGA samples. **B**: Proteasome gene expression level in GTEx samples. **C**:GTEx sample id matched with the TCGA tumour tissue type. **D**:TCGA sample-id corresponding to low and high expression groups of IP. **E**: GTEx sample-id corresponding to low and high expression groups of CP.

Supplementary Table 2: List of different tumour tissues with single-cell transcriptomics data available and their respective references considered in this study.

Supplementary Table 3: Sample level GSVA score of 18 different immune cells across 33 tumour tissue samples from TCGA. These scores were further used for the differential enrichment between high and low proteasome (IP or CP) sample groups.

Supplementary Table 4: Sample level GSVA score of 50 different pathways across 33 tumour tissue samples from TCGA. These scores were further used for the differential enrichment between high and low proteasome (IP or CP) sample groups.

Supplementary Table 5: Proportion of samples having protein affecting mutation in proteasome genes (PSMB5, PSMB6, PSMB7, PSMB8, PSMB9, and PSMB10) at tumour tissue level and at pan-cancer level (last row) in TCGA cohort.

Supplementary Table 6: Cox regression analysis of IP (**A**) and CP (**B**) expression with the overall survival in TCGA cohort. The column represents each variable (and its combination) and the values in the row represent log(hazard ratio(HR)) and adjusted p-value. The cells with no value indicate missing values for that variable in the respective tumour type.

Supplementary Table 7: Description of dataset related to immune checkpoint blockade (ICB) therapy, with the clinical outcome, and the reference details.

Supplementary Table 8: IP and CP expression score in patients samples treated with ICB therapy.

Supplementary Table 9: Gene list for 18 different immune cells, 50 different hallmark pathways, epithelial and mesenchymal gene signatures curated from different sources.